

Tropospheric Aerosol as Reactive Intermediate

Agustín J. Colussi^{1*}, Shinichi Enami^{2,3,4*}, Akihiro Yabushita⁵, Michael R. Hoffmann¹,
Wei-Guang Liu⁶, Himanshu Mishra^{1,6}, and William A. Goddard, III⁶

¹ *Ronald and Maxine Linde Center for Global Environmental Science, California Institute of Technology,*

Pasadena, California 91125, USA

² *The Hakubi Center for Advanced Research, Kyoto University, Kyoto 606-8302, Japan*

³ *Research Institute for Sustainable Humanosphere, Kyoto University, Uji 611-0011, Japan*

⁴ *PRESTO, Japan Science and Technology Agency, Kawaguchi 332-0012, Japan*

⁵ *Department of Molecular Engineering, Kyoto University, Kyoto 615-8510, Japan*

⁶ *Materials and Process Simulation Center, California Institute of Technology, Pasadena, California*

91125, USA

* *Corresponding authors: ajcoluss@caltech.edu enami.shinichi.3r@kyoto-u.ac.jp*

EXPERIMENTAL DETAILS

The formation of nitrate (NO_3^- , $m/z = 62$) on aqueous microjets was investigated by spraying aqueous malonic acid, glutamic acid or glutaric acid solutions into $\text{NO}_2(\text{g})/\text{N}_2(\text{g})$ mixtures at 1 atm, 293 K. Each aqueous solution is injected at $20 \mu\text{L min}^{-1}$ as a liquid microjet *via* an electrically grounded, pneumatic nozzle (bore diameter: 100 μm) into the spraying chamber of an online electrospray ionization mass spectrometry (ESI-MS, HP-1100 MSD), modified with a $\text{NO}_2(\text{g})$ injection system as shown in Supplemental Figure S1.¹ The gas mixture of $\text{NO}_2(\text{g})$ (500 ppm) in $\text{N}_2(\text{g})$ was introduced into the spraying chamber in a direction perpendicular to a stainless steel needle injector and mass spectrometer, respectively. NO_2 concentrations in the chamber were calculated from NO_2/N_2 mixture flow rates as diluted by the N_2 drying gas. Flow rates were regulated by mass flow controllers. This setup is identical to that used in previous studies from our laboratory.¹⁻⁵ The fast nebulizer N_2 gas ($2.65 \times 10^4 \text{ cm s}^{-1}$) shortly tears up the outer layers of the microjet into microdroplets, that are blown up into sub-micron droplets carrying ion excesses of either sign.⁶⁻⁸ The excess charges carried by such sub-micron droplets are necessarily confined to the surface by electrostatics, are not affected by solvent evaporation or by reaction with a neutral gas, and constitute the basic magnitude retrieved as signal intensities by mass spectrometry. Excess ions are ultimately ejected from the surface of rapidly evaporating sub-micron droplets to the gas-phase as a result of electrical repulsion due to charge crowding, selected by an electrically biased inlet port, mass-analyzed and detected within ~ 1 millisecond.¹¹⁻¹³ The ESI-MS signal intensities detected in these experiments are therefore proportional to the amounts of ions of the interfacial layers of nascent microjet that had just reacted with $\text{NO}_2(\text{g})$,³ i.e., prior to its breakup into charged sub-micron droplets.¹⁴ We had verified that this setup actually behaves as a linear transfer device, i.e., ESI-MS signals are directly proportional to ion

concentrations (< 2 mM) in the interfacial layers of the microjet.^{15,16} We have also demonstrated, and reported in the literature, that the products of gas/liquid reactions are formed and remain in the outermost layers of the liquid microjets for their ulterior detection by ESI-MS.³

Typical instrumental parameters were as follows: drying gas temperature, 350 °C; drying gas flow rate, 13 L min⁻¹; Nebulizer pressure, 2 atm; collector capillary voltage, 3.5 kV; fragmentor voltage value, 60 V. All solutions of acids were prepared in MilliQ water (18.2 MΩ cm) from a Millipore Milli-Q gradient water purification system. Solutions pH was adjusted by adding concentrated NaOH solution and measured with a calibrated pH-meter.

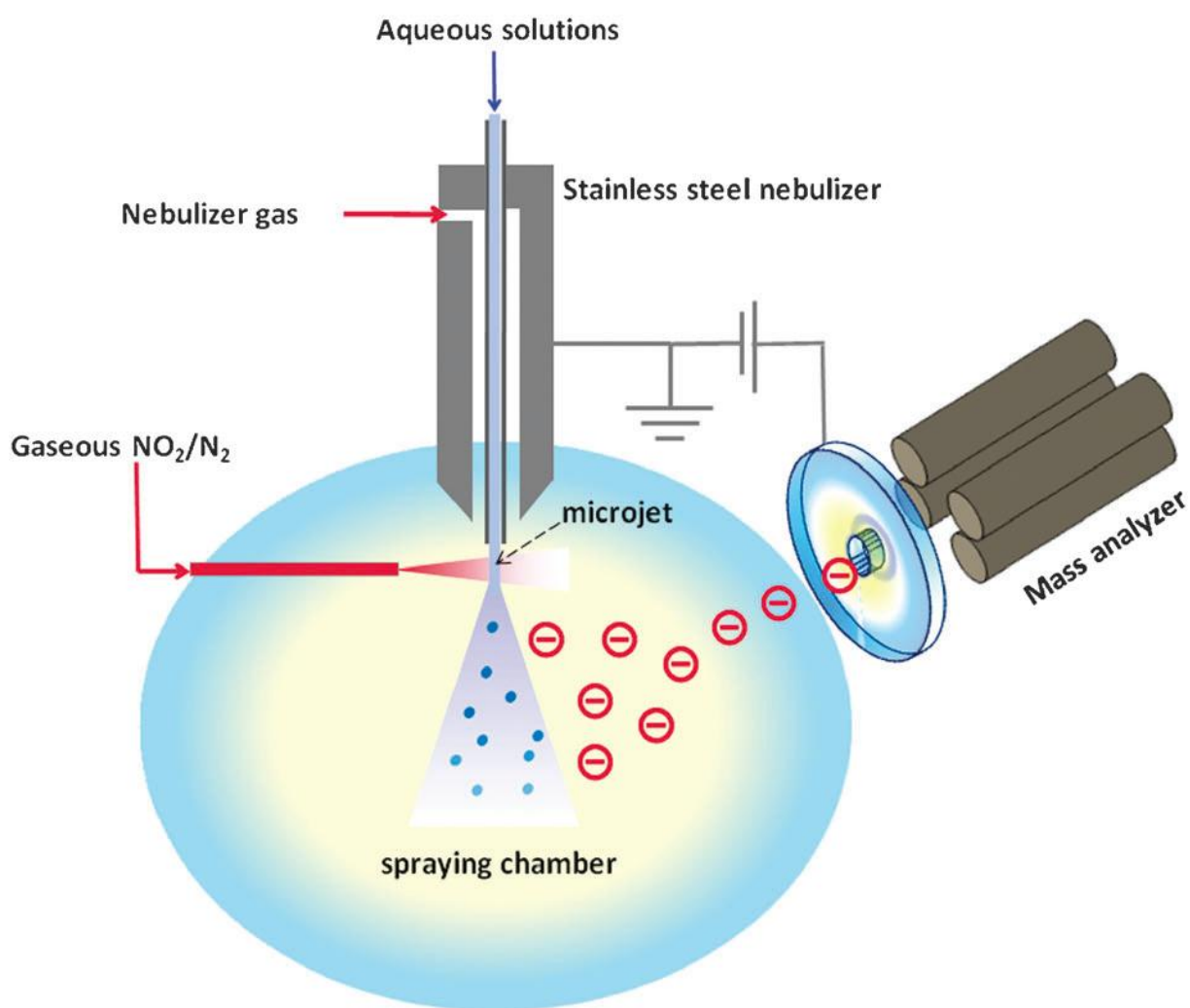


FIGURE S1– Schematic diagram of the spraying chamber with the NO₂(g) injection system

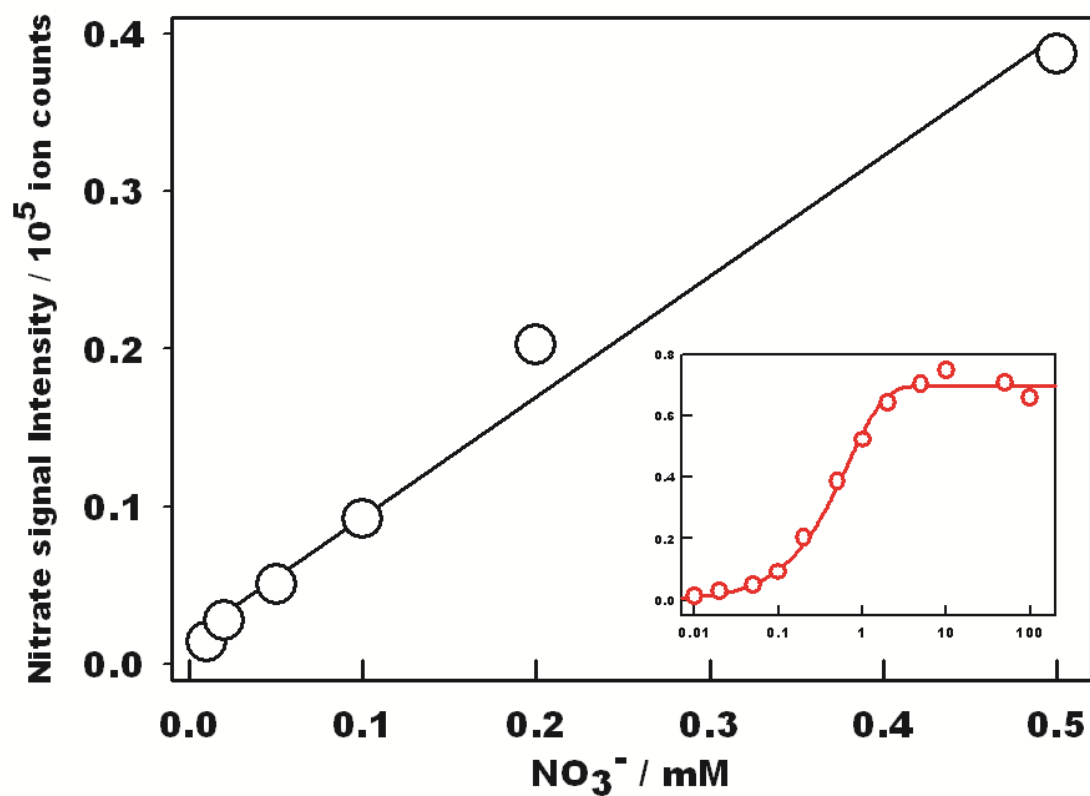


FIGURE S2 – ESI-MS signal intensities of NO_3^- ($m/z=62$) vs. $[\text{NaNO}_3]$ over an extended concentration range display saturation behavior above ~ 2 mM.

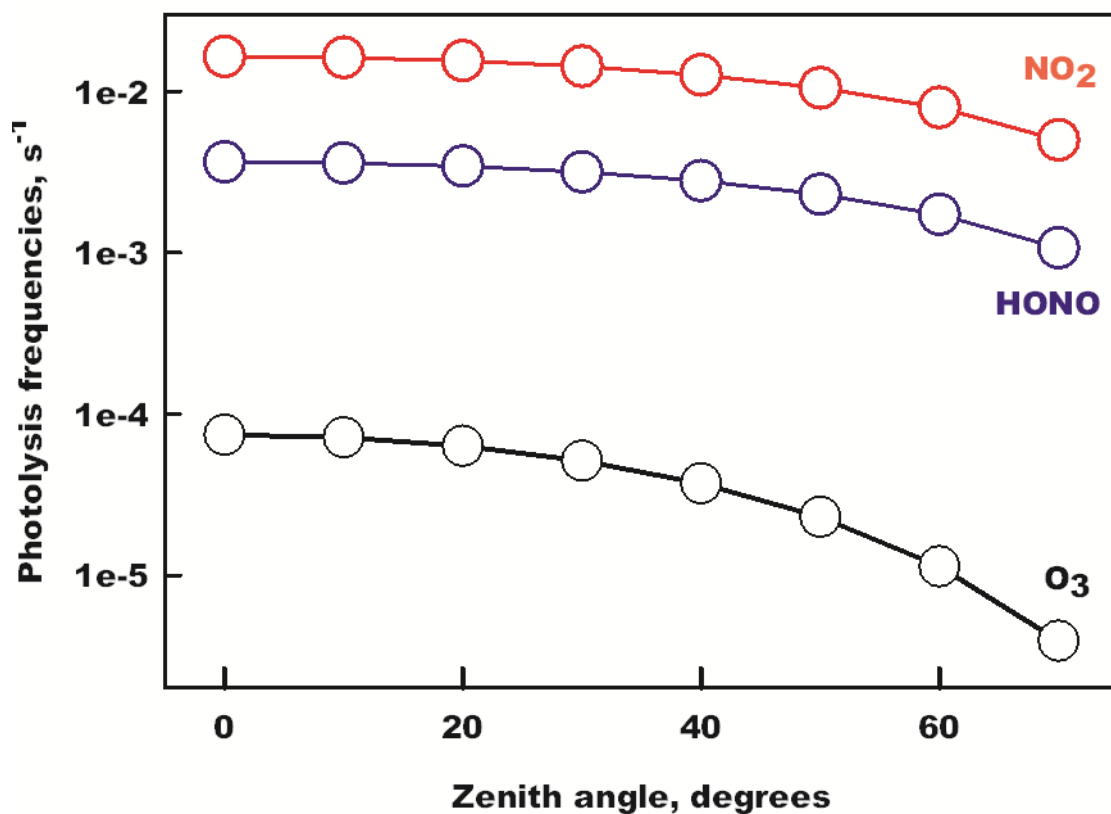


FIGURE S3 – Photolysis frequencies: $J(\text{NO}_2 = \text{NO} + \text{O}^3\text{P})$, $J(\text{HONO} = \text{NO} + \cdot\text{OH})$ and $J(\text{O}_3 = \text{O}_2 + \text{O}^1\text{D})$, as functions of zenith angle at zero elevation, surface albedo 0.4, under an ozone column of 300 Dobson units, at 10 am from Ref. 20 main text.

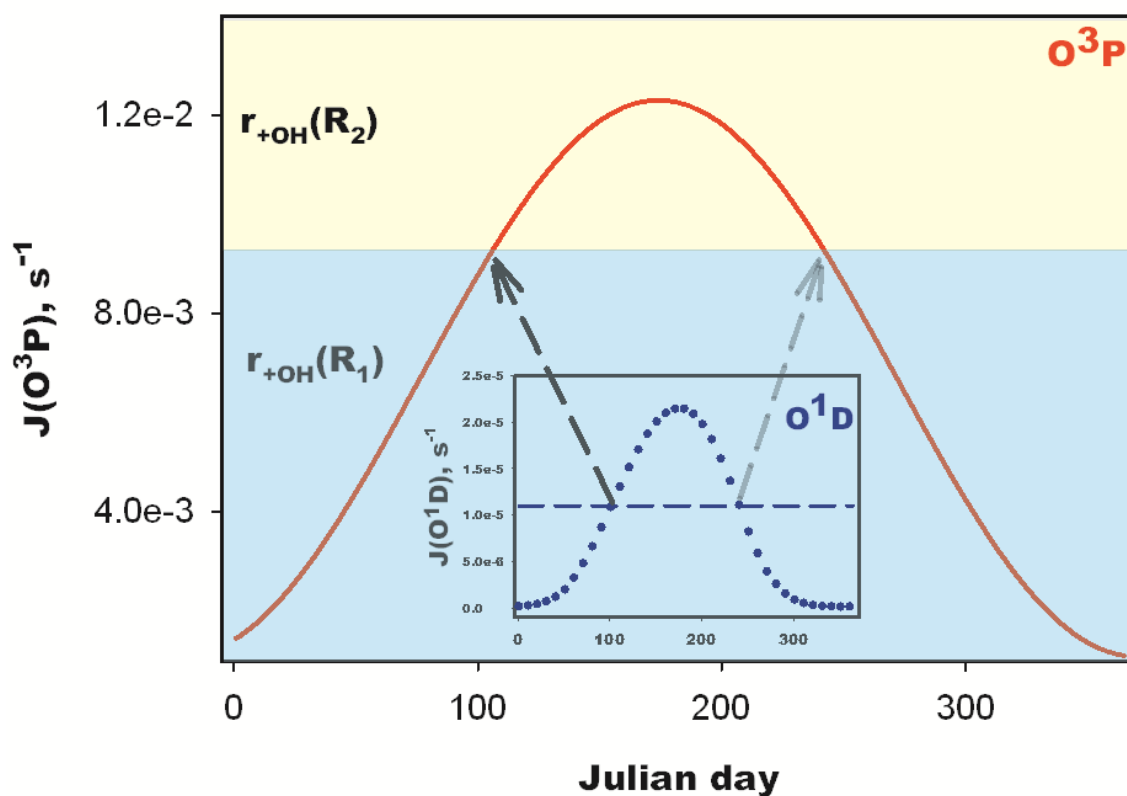


FIGURE S4 – Yearly dependence of the photolysis frequency $J(\text{NO}_2 = \text{NO} + \text{O}^3\text{P})$ over Moscow at zero elevation, surface albedo 0.4, under an ozone column of 300 Dobson units, at 10 am (from Ref. 20). Inset: $J(\text{O}_3 = \text{O}_2 + \text{O}^1\text{D})$ under the same conditions. When $J(\text{O}_3 = \text{O}_2 + \text{O}^1\text{D})$ falls 50% from its peak value, the rate of $\cdot\text{OH}$ production switches from $r_{+\text{OH}}(\text{R}_1)$ to $r_{+\text{OH}}(\text{R}_2)$ at Julian day ~ 100 , and vice-versa at Julian day ~ 240 . See main text, section 8, for further explanations.

REFERENCES

- (1) Yabushita, A.; Enami, S.; Sakamoto, Y.; Kawasaki, M.; Hoffmann, M. R.; Colussi, A. J., *J. Phys. Chem. A*, **2009**, *113*, 4844-4848.
- (2) Kinugawa, T.; Enami, S.; Yabushita, A.; Kawasaki, M.; Hoffmann, M. R.; Colussi, A. J., *Phys. Chem. Chem. Phys.* **2011**, *13*, 5144-5149.
- (3) Enami, S.; Hoffmann, M. R.; Colussi, A. J., *J. Phys. Chem. Lett.*, **2010**, *1*, 1599–1604.
- (4) Enami, S.; Hoffmann, M. R.; Colussi, A. J., *Proc. Natl. Acad. Sci. U. S. A.*, **2008**, *105*, 7365–7369.
- (5) Enami, S.; Hoffmann, M. R.; Colussi, A. J., *J. Phys. Chem. Lett.*, **2010**, *1*, 2374.
- (6) Kebarle, P.; Peschke, M., *Anal. Chim. Acta*, **2000**, *406*, 11–35.
- (7) Nguyen, S.; Fenn, J. B., *Proc. Natl. Acad. Sci. U. S. A.*, **2007**, *104*, 1111–1117.
- (8) Zilch, L. W.; Maze, J. T.; Smith, J. W.; Ewing, G. E.; Jarrold, M. F., *J. Phys. Chem. A*, **2008**, *112*, 13352–13363.
- (9) Kahen, K.; Jorabchi, K.; Gray, C.; Montaser, A., *Anal. Chem.*, **2004**, *76*, 7194.
- (10) Dodd, E. E., *J. Appl. Phys.*, **1953**, *24*, 73–80.
- (11) Fenn, J. B., *J. Am. Soc. Mass Spectrom.*, **1993**, *4*, 524–535.
- (12) Fenn, J. B., *Angew. Chem., Int. Ed.*, **2003**, *42*, 3871–3894.
- (13) Nguyen, M. L.; Bedjanian, Y.; Guilloteau, A., *J. Atmos. Chem.*, **2009**, *62*, 139–150.
- (14) Enami, S.; Hoffmann, M. R.; Colussi, A. J., *J. Phys. Chem. B*, **2008**, *112*, 4153–4156.
- (15) Cheng, J.; Psillakis, E.; Hoffmann, M. R.; Colussi, A. J., *J. Phys. Chem. A*, **2009**, *113*, 8152–8156.
- (16) Enami, S.; Vecitis, C. D.; Cheng, J.; Hoffmann, M. R.; Colussi, A. J., *J. Phys. Chem. A* **2007**, *111*, 8749–8752.